Title
Fibromodulin and Its Derivative Reduce Scars in Adult Porcine Models

Author
Chen, Yao

Publication Date
2016

Peer reviewed|Thesis/dissertation

UNIVERSITY OF CALIFORNIA

Los Angeles

Fibromodulin and Its Derivative Reduce Scars in Adult Porcine Models

A thesis submitted in partial satisfaction

of the requirements for the degree

Master of Science in Oral Biology

by

Yao Chen

2016

ABSTRACT OF THESIS

Fibromodulin and Its Derivative Reduce Scars in Adult Porcine Models

By

Yao Chen

Master of Science in Oral Biology

University of California, Los Angeles, 2016

Professor Kang Ting, Chair

Background: Cutaneous fibrosis (scar formation) is a significant clinical problem which leads to a lot of developmental, functional, aesthetic, and psychological difficulties[1]. Current therapeutic strategies for the scars and hypertrophic scars are minimally effective or have undesirable adverse effects such as reduced wound strength, delayed healing, and skin atrophy caused by corticosteroids[2]. Therefore, an alternative solution for combatting scar formation with improved efficacy and decreased adverse effects needs to be developed. Through a sustained, 15-year research effort examining wound healing, we identified fibromodulin (FMOD) as a prerequisite for fetal scarless skin. FMOD also accelerates wound closure, promotes angiogenesis, decreases scarring, and improves extracellular matrix (ECM) organization in adult mouse models. Furthermore, we developed a 40 amino acid FMOD-based peptide sequence, F06-C40, which has similar pro-migration/contraction effect as full-length FMOD in mouse models while being more efficient and less costly to produce. However the anti-scar effect of FMOD and peptide has not been confirmed in large animal models. In this study, the effect of FMOD and F06-C40 on scars and hypertrophic scars was tested in porcine models for future preclinical studies.

Methods: To investigate the anti-scar effect of FMOD and its peptide F06-C40, full-thickness incisional wounds (1.5 cm x 0.5 cm) were generated on the dorsum of Yorkshire pigs or red Duroc pigs to simulate human normal scarring or hypertrophic scarring, respectively. High-tension wounds with 4-fold increase in tension compared with a normal wound were also created on the back of red Duroc pigs to generate high-tension wound models. 2.0 mg/ml FMOD, different dosages of F06-C40 (10mg/ml,

25mg/ml, and 50 mg/ml), or PBS control buffer were injected intradermally around the wound edge (100 µl x 2 edges = 200 µl total/wound), via single or double injections. At 8 weeks post-injury, scar formation was evaluated by gross appearance visual assessment, histological analysis such as H&E staining, Masson's Trichrome staining, Picrosirius red staining (PSR) coupled with polarization microscope (PLM) or confocal laser scanning microscope, and tensile strength measurement.

Results: FMOD and F06-C40 peptide significantly reduced scar formation in both Yorkshire pig and red Duroc pig models. Visually, the gross appearance of scars was pronouncedly improved in FMOD- or F06-C40-treated wounds. Histologically, the ECM organization was improved, and scar area was reduced with the injection of FMOD or F06-C40. In addition, scar tensile strength at 8 weeks post-injury was increased after treating with FMOD or F06-C40.

Conclusion: FMOD and F06-C40 both present the anti-scar effect on pig models, which are the FDA regulatory gold standard for wound healing studies. The results from this preclinical study indicate that F06-C40 have the potential to be developed as a novel therapeutic for improving wound healing in normal scarring and hypertrophic scarring patients.

The thesis of Yao Chen is approved

Reuben Kim

Shen Hu

Tara Aghaloo

Kang Ting, Committee Chair

University of California, Los Angeles

2016

This thesis is dedicated to

All of the mentors for their academic guidance

the entire lab mates who have contributed to this project

and my family and friends

who have supported me throughout my life

TABLE OF CONTECTS

LIST OF FIGURES

Acknowledgements

This study was supported by the Plastic Surgery Foundation® (2013 National Endowment for Plastic Surgery 269698), NIH-NIAMS (R43AR064126, R44AR064126, and R43AR063558), NIH-NIDCR (R44DE024692). CLSM was performed at the Center for NanoScience Institute Advanced Light Microscopy/Spectroscopy Shared Resource Facility at UCLA, which was supported by funding from NIH-NCRR shared resources grant (CJX1-443835-WS-29646) and NSF Major Research Instrumentation grant (CHE-0722519).

Fibromodulin and Its Derivative Reduce Scars in Adult Porcine Models

INTRODUCTION

Cutaneous fibrosis (scar formation) is a significant clinical issue which leads to developmental, functional, aesthetic, and psychological difficulties to patients. It affects up to 100 million people and results in over 55 million operations per year, which translate to annual costs approaching $3 billion[1]. Cleft lip and palate (CLP) is the most common craniofacial congenital anomaly present at birth, occurring at a rate of 79.1 per 100,000 live births in the US[3]. The repair of cleft lip can result in hypertrophic scar formation, which is significantly more challenging than other scars and requires multiple surgical revisions due to the lack of tissue and the excessive tension. Unfortunately, current methods for the prevention and treatment of scars and hypertrophic scars are minimally effective or have undesirable adverse effects, such as reduced wound strength, delayed healing, and skin atrophy caused by corticosteroids[2]. Thus, an alternative potential solution for combatting scar formation with improved efficacy and decreased adverse effects needs to be developed.

A cutaneous scar is fibrous tissue that replaces normal dermis after trauma or surgery, which is a natural part of wound healing process that results from the skin and other tissue wound repair. It involves the resolution of wounds rather than skin regeneration[4]. During the formation of scars, it undergoes significant macro- and microscopic changes, such as pigmentation, fibroblast proliferation and collagen deposition[4-6]. Scar tissues lack sweat glands and hair follicles. Mainly, scar tissues consist of disorganized collagenous extracellular matrix. Instead of a random

basket-weave-like pattern formation of collagen fibers in normal skin, the formation of collagen fibers in scar tissues are pronouncedly aligned in a single direction[7,8]. In addition, the architectural organization of collagen has distinct changes in scar tissues with higher collagen density and smaller collagen bundle size[8,9].

Hypertrophic scarring, one of the most common types of cutaneous scars, is a serious clinical problem and a suboptimal consequences of skin wound healing[10]. It occurs after deep dermal wounds such as cuts, burns, trauma, abrasion[11], which involves the overproduced collagen, excessive dermal fibrosis and a decrease in small leucine-rich proteoglycans during wound healing process[4,12-14], and can be followed with permanent dermal functional loss and stigma of disfigurement[12,15]. The mechanical tension on a wound has been identified as a leading cause for hypertrophic scar formation. The hypertrophic scars appear as raised, thickened, red and itchy, firm lesions that are confined to edges of original wound, but may continue to thicken for up to six months[4,15]. The architectural pattern of collagen in hypertrophic scars has unique characteristics which contains nodules of collagen and is highly compact[16]. The distinctive feature of the formation of collagenous nodules composed of tightly packed collagen decides it challenging to cure.

Scar tissues caused by injury or surgery result from the changes in skin structures and compositions. To successfully evaluate the scar formation after injury, scar tissues should be assessed in different ways. Subjective and objective visual assessment of scar appearance directly shows wound healing degree but offers only limited insight. Histologically, Hematoxylin and eosin staining (H&E) is commonplace and useful in visualizing epidermal, dermal and subcutaneous features of a biopsy[17]. In order to

directly observe scar formation, Masson's Trichrome staining can be used for fibrotic scarring to identify scar tissues and morphology changes[18-21]. In addition, picrosirius red (PSR) staining procedure with polarization microscope (PLM) is another commonly used histological technique to stain collagen fibers and visualize collagen content and morphology[22,23]. The autofluorescent property of PSR stained collagen can be used for confocal microscope images, which has high throughput analysis of collagen with higher magnification. Tensile strength is one of the crucial indices for skin and scar biomechanics, which identifies tissue's physiologically relevant viscoelastic behavior and resistance to rupture[24]. In this study, different methods were used to thoroughly evaluate the degree of scar formation in the animal models.

To successfully achieve clinical translation, a proper selection of an animal model similar to human skin is crucial. Small mammals such as mice, rats, and guinea pigs are commonly used for wound healing studies due to the availability and cost[25-28]. However, they have many differences from human skin both anatomically and physiologically, including the relatively thinner epidermis, significantly higher epidermal appendage density with different hair follicles from human's, and higher contraction property in rodent models[29,30]. Moreover, these animal models have all failed to generate scars that are analogous to human hypertrophic scars[13]. Pigs have been used to study many diseases with over 1500 publications due to the similarities to human, such as diabetes, infections, and cardiovascular diseases[31-33]. Pig skin is the FDA regulatory gold standard for wound healing[13]. Anatomically, pig skin has more similar structures such as thick epidermis, distinct rete pegs, dermal papillae and similar dermal collagen with human skin. Physiologically, the wound healing processes are comparable between human and

pigs, as well[29,30]. In cutaneous wound healing, pig models show much more concordance (78%) with human studies, compared with only 53% concordance in other animal models[29]. Thus, pig models are perfect for clinical translation in wound healing studies because of the similarities to human skin with respect to structure, mechanical properties, and wound healing. Female Yorkshire pigs and Red Duroc pigs are reported to be the most commonly used pig models for wound healing studies. The cutaneous scarring in female red Duroc pig has a lot of similarities with human hypertrophic scarring. Partial thickness wounds in female red Duroc pigs healed with hypertrophic scarring have been reported decades ago[34]. The partial-thickness burn wounds generated in red Duroc pig models are comparable with human hypertrophic scars in which deep dermis remains as is the case in burn injuries, unlike that in small mammal models which can only generate small, full-thickness wounds[15]. Female red Duroc pigs can be generated with thick healed wounds, which are analogous to human hypertrophic scars. The collagen patterns in the red Duroc pig model wounds are disorganized and formed into nodules[15]. Both visually and histologically, female red Duroc pigs are perfect models to study hypertrophic scars. Therefore, in this study, Yorkshire pigs were used to study normal wound healing process in cutaneous scars, while red Duroc pigs were used to study the wound healing in hypertrophic scars.

Fibromodulin (FMOD) is a 59kDa protein broadly distributed small leucine-rich proteoglycan (SLRP), which plays an essential role in cutaneous wound repair[35-38]. It is a collagen-binding protein that can be found widely in many types of connective tissues such as cartilage, tendon, and skin; especially, it is present in the epidermis of human skin and expressed by human keratinocytes in culture[36]. It has been shown that FMOD

interacts with type I and type II collagen fibrils and inhibits fibrillogenesis *in vitro*; thus, it may play a role in the assembly of extracellular matrix[39,40]. Decades ago, it has already been demonstrated that collagen fiber bundles appeared abnormally in FMOD-null mice. In tendon, the tissue organization and lumican deposition were altered[41]. In addition, FMOD has the ability to modulate transforming growth factor-beta (TGF-β) activities by sequestering TGF-β into the extracellular matrix. The increased level of FMOD may partly affect scarless fetal repair through decreased TGF-β bioavailability[37]. FMOD is also a target gene of FBLN5 and has the capacity to reduce nuclear factor-κb (NF-κB) activity by delaying the constitutive degradation of IκBα via a JNK-dependent pathway that promotes the activation of c-Jun N-terminal kinase, the inhibition of calpain and casein kinase 2 activity, and the induction of fibroblast apoptosis[42]. Through a sustained, 15-year research effort examining wound healing, our lab identified FMOD as a prerequisite for fetal scarless skin with anti-scar properties. Previous studies have shown that FMOD is highly expressed in wound healing process and the analyses of fibromodulin-deficient (*Fmod*$^{-/-}$) mice have confirmed that FMOD is essential for fetal scarless wound healing and normal adult wound healing[37,43]. In addition, intradermal recombinant human (rh) FMOD protein injection significantly reduces scar size to 50%-70% of the original scar size in primarily closed wounds in mouse wound models. FMOD is a novel molecule that has the ability to accelerate wound closure, promote angiogenesis, decrease scarring and improve extracellular matrix (ECM) organization and wound tensile strength in adult mouse wound models[8,37,43-45]. At the cellular level, the application of FMOD significantly up-regulates fibroblast activation, migration and invasion *in vitro*. PCR array data showed the increase expression of fibroblast activation

and migration/adhesion genes such as connective tissue growth factor (*CTGF*), *ACTA2*, matrix metalloproteinase (*MMP*)-2 and -1[46-48]. Moreover, FMOD significantly decreases expression of pro-fibrotix growth factor TGF-β1 and fibrillar collagens type I and type III. The significant anti-fibrotic effects of FMOD make it a promising treatment for scar healing. However, FMOD is inefficiently produced in bacteria and yeast systems[49], expensive mammalian cell culture is the mainstay for FMOD whole protein manufacturing, which causes significant cost, especially if cells have low yields, or if multiple purification columns are required. Recently, a 40 amino acid long FMOD-based peptide sequence, F06-C40, which is similar to the amino acid full FMOD protein in its anti-fibrotic effects, has been developed. It retains the same anti-fibrotic effects and similar cellular effects as FMOD whole protein in mouse wound models, but without glycosaminoglycan side chains, which is short enough to be manufactured using a peptide synthesizer. Previously, the anti-scar efficacy of F06-C40 has been confirmed with mouse models.

In this study, different pig models were used to investigate the role of FMOD protein and FMOD-derived peptide, F06-C40, in wound healing. Additionally, the dosage of F06-C40 was optimized in pig models for future clinical studies.

MATERIALS AND METHODS

2.1 Animal surgery procedures

All animal surgeries were performed under institutionally approved protocols provided by the Chancellor's Animal Research Committee at UCLA (protocol number: 2008-016).

2.1.1 Primary closure wound porcine models

Primary closure wound porcine models were used in this study to simulate adult human wound healing[50]. Briefly, 20-kg female Yorkshire pigs (S&S Farms) or red Duroc pigs (Pork Power Farms) were sedated with Telazol® (Tiletamine and Zolazepam, Fort Dodge Lab) 5 mg/kg intramuscular injection. The pigs were then intubated endotracheally and maintained under a surgical plane of anesthesia with isoflurane at 0.5-2.5% in room air. The flank and back hair were clipped and the skin was sterilely prepared with three alternating scrubs of povidone iodine solution and alcohol. Full-thickness wounds were created with a #15 surgical blade by excising a 1.5 cm x 0.5 cm ellipse of skin with its long axis running perpendicular to the lines of minimal tension, down to the level of the panniculus carnosus. All wounds were separated by at least 2 cm to minimize adjacent wound effects. Each open wound edge was intradermally injected with FMOD, F06-C40 or control buffer at the time of surgical wound closure only for the one-time injection group. Wounds were then marked with permanent dye and closed primarily with 3-0 Nylon mattress sutures. Additional injection was performed into each edge of the wound 24 hours later. Sutures were removed at 2 weeks post-injury

and wounds were harvested at 4 or 8 weeks post-injury. Unwounded skin tissues distant from the wounds of each animal were also collected as controls.

2.1.2 High-tension wound porcine models

Identical anesthesia methods were used in high-tension wound porcine models as described above. Full-thickness wounds were created by excising a 1.5 cm X 2.0 cm ellipse of skin to generate high-tension wound models. All wounds were separated by at least 2 cm to minimize adjacent wound effects. Each open wound edge was intradermally injected with FMOD, F06-C40 or control buffer at the time of surgical wound closure only for the one-time injection group. Wounds were then marked with permanent dye and closed primarily with 3-0 Nylon mattress sutures. A total of 24 wounds were created in each animal. Sutures were removed at 2 weeks post-injury and wounds were harvested at 8 weeks post-injury (N = 6 wounds from 2 red Duroc pigs per treatment).

2.2 Scar visual appearance evaluation

Gross visual assessment of the scar was performed with an adaption of Visual Analogue Scale (VAS) scoring as described previously[51]. Briefly, all scar images were taken by a highly sensitive digital camera (Canon DSLR DS126181, Canon, Japan), and presented in a screen, each for a maximum of 20 seconds, to 3 experienced MD assessors. The assessors placed a mark on a horizontal, 100-mm line to represent the scar quality, with 0 indicating normal skin and 100 indicating a poor scar (**Fig. 1A and 1B; Fig. 4**). When the individual images were displayed, the assessors documented and

were asked to confirm a VAS.

2.3 Histological analysis

After fixation, skin samples were dehydrated, paraffin-embedded, and sectioned at 5-μm increments for H&E staining, Masson's Trichrome staining, or 10-μm for PSR staining. For systematic calculation of scar size, we developed a histomorphometric Scar Index that took into account both scar area and dermal thickness. Scar Index (SI) was used to standardize measurements of scar formation relative to skin thickness, which differs among animal models[8,43]. SI was calculated by dividing the scar area (A) by the corresponding average dermal thickness (T_{avg}); SI = A/T_{avg} (**Fig. 1C**). H&E staining photographs were captured on an Olympus BX51 microscope (Olympus America Inc., Center Valley, PA) equipped with MicroFire 2.2 digital camera (Optronics, Goleta, CA) using PictureFrame 2.0 software (Optronics) at 40× magnification. Image analysis was performed using the NIH program ImageJ.

2.4 Confocal laser scanning microscopy (CLSM)

Following PSR staining, the dermal collagen deposition pattern of the upper dermis was evaluated by confocal microscopy on a Carl Zeiss LSM 510 META Laser scanning confocal microscope by previously published methods[8,43].

2.5 Tensile strength measurement

Tensile strength was determined using an Instron 5565 Universal Testing Machine (Instron). For pig skin, an exact 4 cm x 1 cm full-thickness skin strip was obtained by

meticulous dissection, with the wound exactly bisecting the sample. Pneumatic compression grips were used to avoid slippage of the specimen. A 1-cm square area of skin was clamped on either side of the wound. The load to failure [breaking strength, as measured in Newtons (N)] was recorded.

2.6 Local toxicity studies

Yorkshire pigs were used to minimize animal sacrifice and to simulate actual scar revision surgery. 1.5-cm length (0.5-cm width) primarily closed wounds were treated with F06-C40 at times 0 and 24 hours by intradermal injection. We locally tested F06-C40 concentrations up to 50 mg/ml with 0.3 ml applied for 1.5-cm linear wound (10 mg F06-C40 per 1 cm of wound length). Clinical observation and body weight were assessed daily in 12 weeks.

2.7 Statistical analysis

All statistical analyses were conducted per consultation with the UCLA Statistical Biomathematical Consulting Clinic. Initial animal numbers were on the basis of an $\alpha = 0.05$, power = 0.8. Statistical analysis was computed by OriginPro 8 (Originlab Corp., Northampton, MA). Data were generally presented as mean ± the standard deviation. $P < 0.05$ was considered statistical significance. One-way ANOVA and two-sample *t*-test were used to compare results of two groups. Individual comparisons between two groups were determined by the Mann-Whitney test for non-parametric data.

RESULTS

3.1 FMOD and its derivative significantly reduce scar formation in adult Yorkshire pig wound models.

Pig models are required by the Food and Drug Administration (FDA) for human skin product testing because among mammalian skins, porcine skin most closely approximates human skin in anatomic structure, mechanical properties, and wound healing[13,29,30]. Yorkshire pigs were used in our study to test the anti-scarring effect of FMOD and its derivative, F06-C40, on normal scarring. FMOD application improved the gross appearance of Yorkshire pig wound at 8 weeks post-injury as assessed by the Visual Analogue Score (VAS) **(Fig. 1A-1B; 2A-2B)**. FMOD treated Yorkshire pig groups also exhibited significantly reduced scar size compared with control (phosphate buffered saline; PBS) at 4 and 8 weeks post-injury **(Fig. 2A and 2C)**. Importantly, the reduced scar size did not occur at the expense of diminished tensile strength. In fact, tensile strength was significantly increased in all FMOD-treated groups relative to controls at 4 and 8 weeks post-injury **(Fig. 2D)**. Dermal collagen architecture was also significantly more organized in the FMOD-treated groups **(Fig. 2A)**.

F06-C40 peptide, a FMOD derivative, was also utilized to assess the anti-scarring effect on Yorkshire pig wound models. The injection of 2.0-mg/ml F06-C40 significantly reduced scar formation; however, the tensile strength of scars after low dose of F06-C40 was not ideal (*data not shown*). Therefore, different concentrations (10 mg/ml, 25 mg/ml, and 50 mg/ml) of F06-C40 were applied to optimize the dose and regimen for porcine wound healing. The scar gross appearance was significantly improved in all

F06-C40-treated groups compared with PBS treatment at 8 weeks post-injury **(Fig. 3A, 3D)**. Scar size was significantly decreased in F06-C40 treatment with both one injection and two injections **(Fig. 3B, 3C)**. Scar Index assessment **(Fig. 3E)** was correlated with histological analyses to further confirm the scar size reduction by F06-C40; and biomechanical testing that revealed that F06-C40 treatment significantly increased the primary outcome of wound tensile strength maintenance **(Fig. 3F)**. F06-C40 pronouncedly reduced scar formation in Yorkshire pigs and increased wound tensile strength while the scar reduction had no difference in all F06-C40-treatment groups, indicating 10mg/ml F06-C40 with one injection post-injury can be the optimized dose for porcine wound healing.

Fig. 1. Scar gross appearance criteria for adult Yorkshire pig wounds.

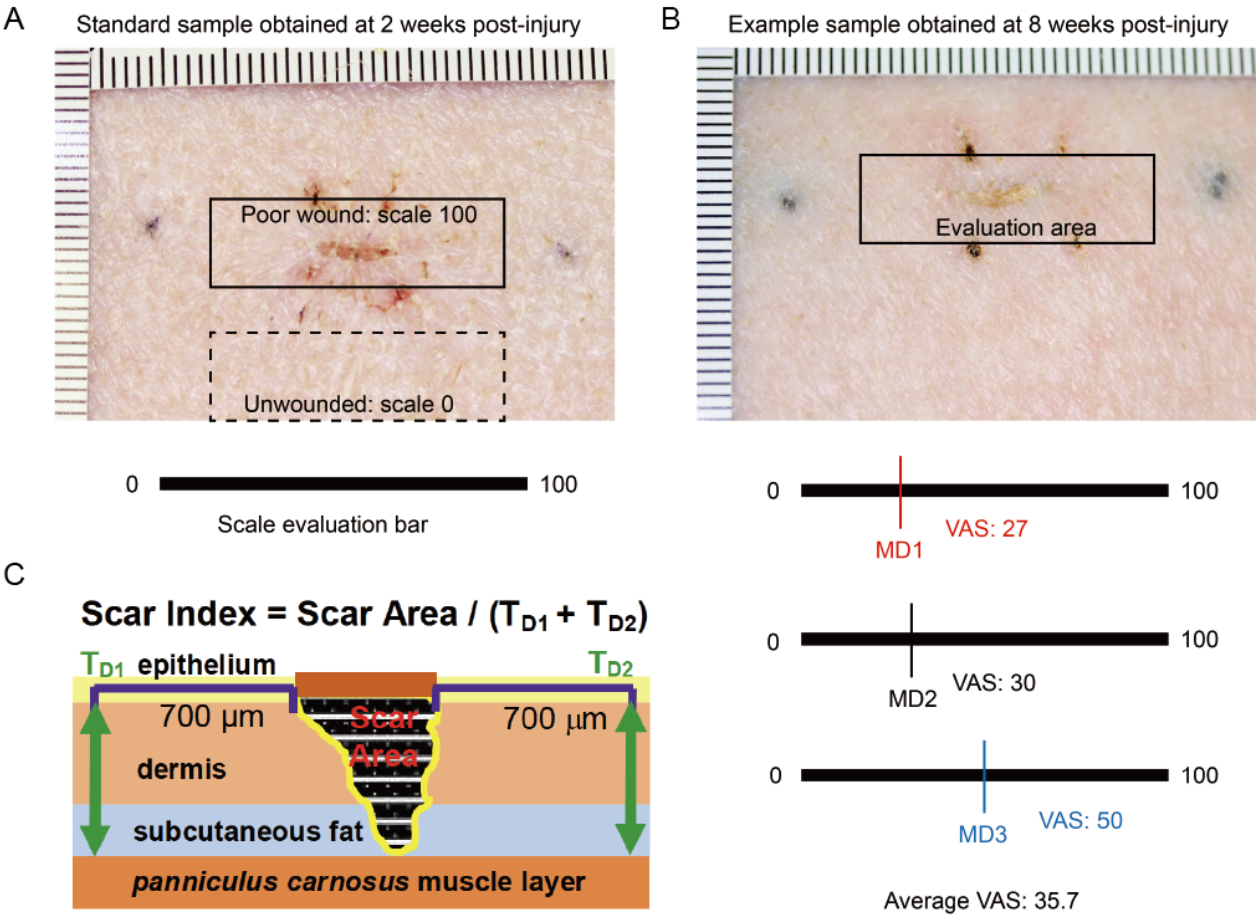

Fig. 1. Scar gross appearance criteria for adult Yorkshire pig wounds. (A) VAS scoring of scar appearance was determined by three-blinded MD reviewers from 0 to 100 based on the wound healing condition. **(B)** The example sample for VAS scoring. **(C)** Schematic image illustrating the measurements used for scar size analysis. Two dermal thickness measurements were taken 700 μm away from the left and right wound edges (T_{D1}, T_{D2}) per sample. To obtain scar size, fibrotic scar tissue area was outlined using the freeform outline tool in ImageJ and was measured to extend from the base of the epidermis to the panniculus carnosus. Scar Index was calculated by dividing the scar area by the corresponding average dermal thickness.

Fig. 2 FMOD reduces scar formation in adult Yorkshire pig wounds.

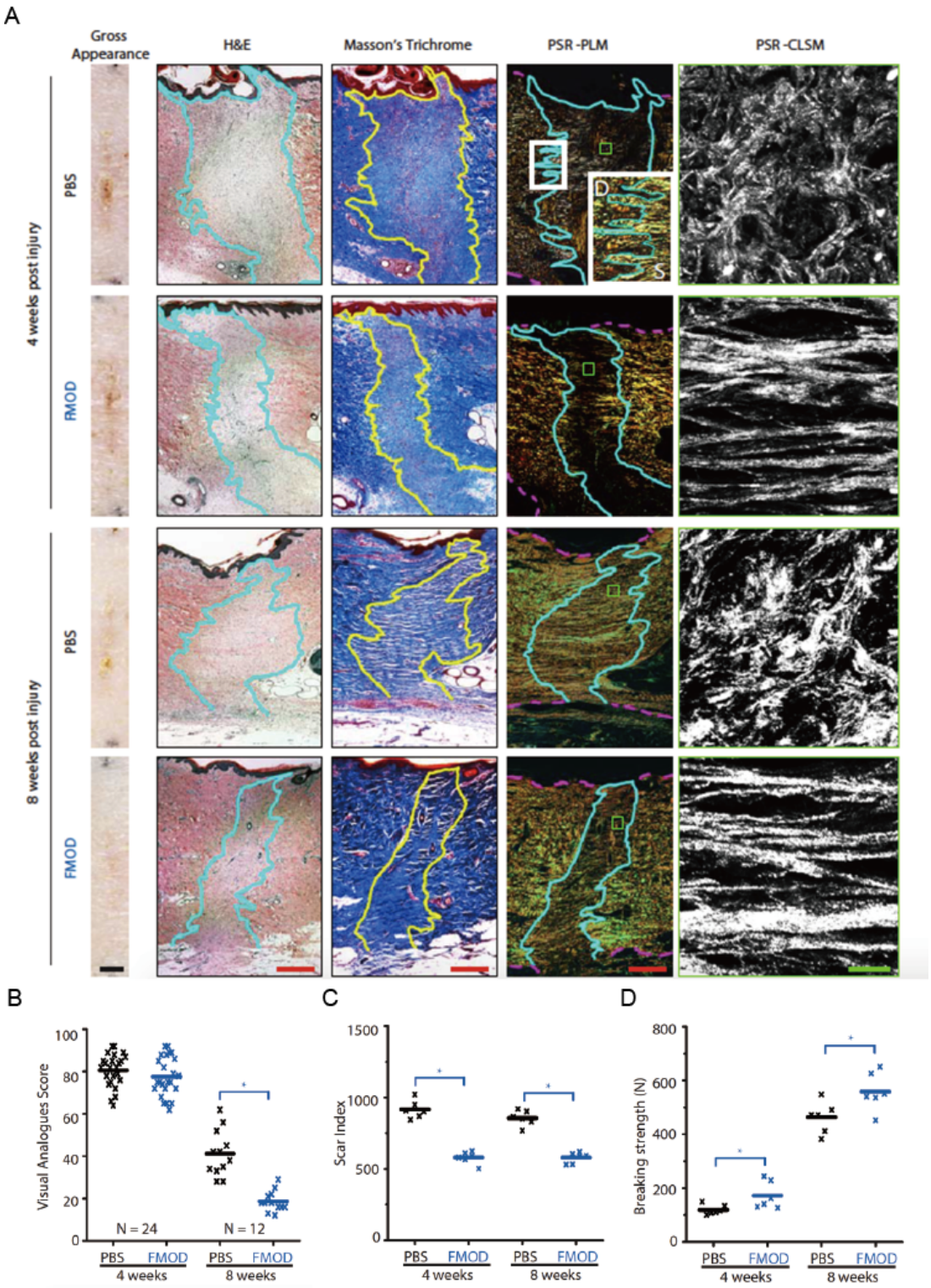

Fig. 2. FMOD reduces scar formation in adult Yorkshire pig wounds. Representative photographs of gross appearance, H&E staining, Masson's trichrome staining, PSR-PLM, and PSR-CLSM of adult Yorkshire pig wounds at 4 and 8 weeks post-injury are shown **(A)**. Compared with H&E and trichrome staining, PSR-PLM distinguished more clear boundaries between scar tissue (S; right) and unwounded normal dermis (D, left) as evidenced in the inset at higher magnifications. Compared with PBS-treated wounds, 2.0 mg/ml FMOD-treated wounds exhibited improved gross appearance (evidenced by decreased Visual Analogous Score; **B**), reduced scar size (scar index) **(C)**, and increased wound tensile strength **(D)**. Scar tissues outlined by cyan lines, while dermis layers outlined by dashed magenta lines on PSR-PLM photographs. Scale bar = 2.5 mm (black), 500 μm (red), or 25 μm (green), respectively. N = 24 (B, 4 weeks post-injury), 12 (B, 8 weeks post injury), or 6 (C and D) wounds from 3 pigs per time point. *$p < 0.05$.

Fig. 3. F06-C40 reduces scar formation in adult Yorkshire pig wounds.

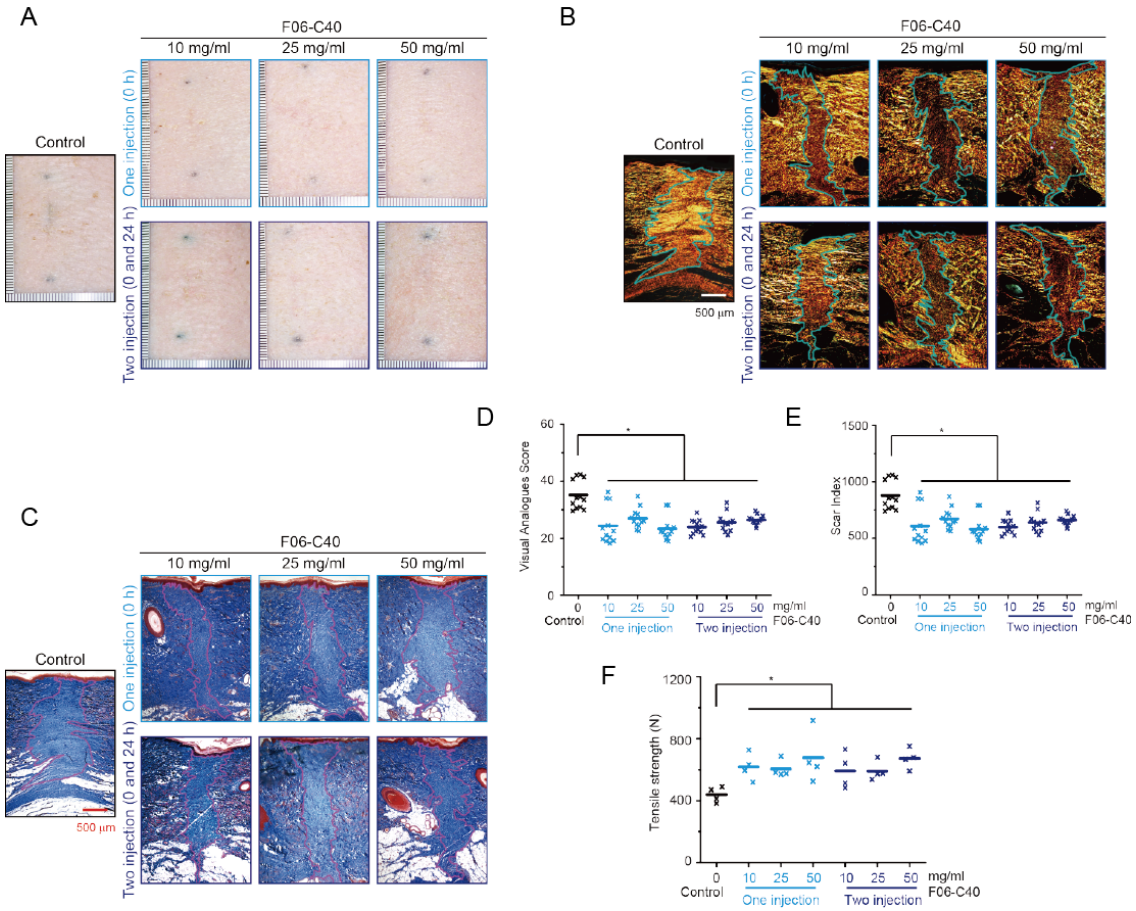

Fig. 3. F06-C40 reduces scar formation in adult Yorkshire pig wounds. 1.5-cm length (0.5-cm width) primary closed wounds were created on adult female Yorkshire pig dorsal skin. 100 µl of 10, 25, or 50 mg/ml peptide was intradermally injected into each wound edge at time 0 only for one-injection group and another 50 µl 24 hours later for two-injection group. **(A)** Representative scar appearance at 8 weeks post-injury. **(B)** Picrosirius red (PSR)-polarized microscope (PLM) images at 8 weeks post-injury. **(C)** Masson's Trichrome staining **(D)** Visual Analogue Scale (VAS) scoring of scar appearance as determined by three blinded MD reviewers. **(E)** Quantification of scar size (SI) and **(F)** tensile strength testing at 8 weeks. Single or double injections and concentrations above 10 mg/ml demonstrated no significant difference in scar improvement. N = 12 wounds per treatment, N = 7 pigs. *$p < 0.05$.

3.2 FMOD and its derivative reduce hypertrophic scarring in red Duroc pig models.

In order to rigorously test the anti-scarring effects of FMOD in a model more relevant to human wound healing, we excised and primarily closed skin wounds in not only Yorkshire, but also red Duroc pigs, which model human pathologic hypertrophic scarring[50]. The identical experiments in Yorkshire pigs were repeated in red Duroc pig models. Although no animal model completely reproduces human hypertrophic scarring, red Duroc pigs more closely simulate human fibroproliferative/hypertrophic scarring than other available models[13,50]. Excitingly, FMOD demonstrated similar efficacy in the red Duroc pig models as in the Yorkshire models. At 8 weeks post-injury, scar gross appearance was evaluated with VAS as **Fig. 4**. FMOD treatment significantly improved gross scar appearance and reduced scar size compared with control (PBS; **Fig. 5A-5D**). Meanwhile, tensile strength and collagen organization were significantly enhanced with FMOD treatment (**Fig. 5C and 5E**). These studies on porcine wound healing indicated that FMOD reproducibly reduces scar size while increasing tensile strength and improving dermal collagen architecture in FDA-required preclinical large animal models.

F06-C40 was applied to red Duroc pigs as well. The optimized concentration of F06-C40 was based on the anti-scarring studies using Yorkshire pigs. F06-C40 application significantly improved the visual appearance of scars at 8 weeks in red Duroc pigs, as shown by the PSR-polarized microscope and quantified using VAS **(Fig. 5A-5C)**. These results were confirmed by scar size quantitation, which showed that 10 mg/ml F06-C40 achieved a striking 51% scar size reduction and significantly increased wound breaking strength by 40% **(Fig. 5D and 5E)**.

Fig. 4. Scar gross appearance criteria for adult red Duroc pig wounds.

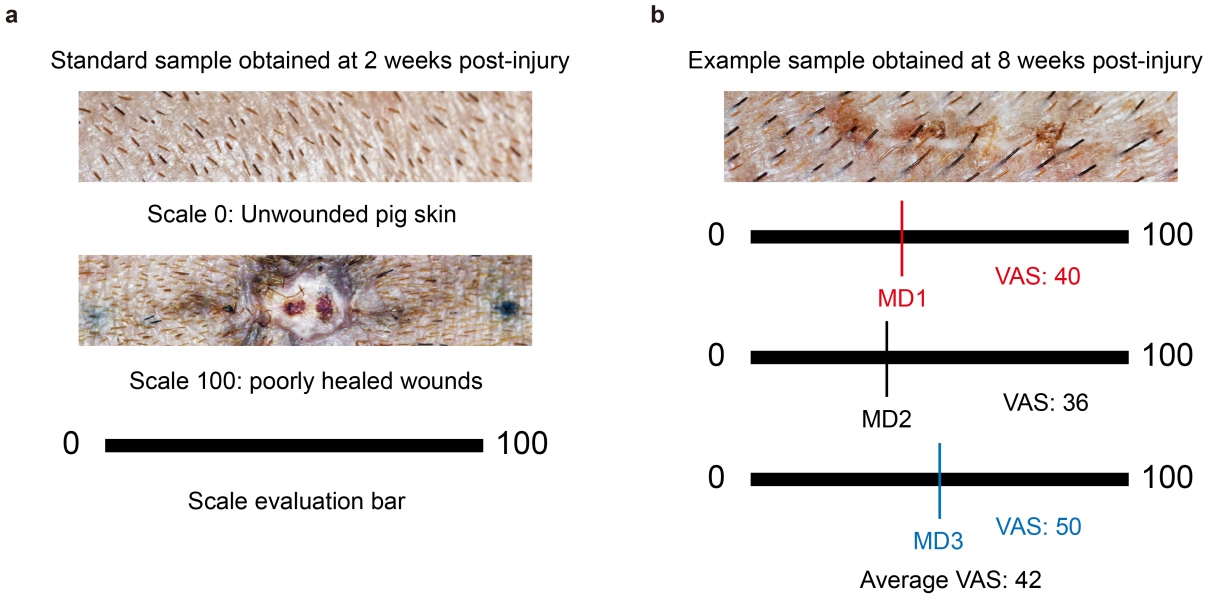

Fig. 4. Scar gross appearance criteria for adult red Duroc pig wounds. (A) VAS scoring of scar appearance was determined by three-blinded MD reviewers from 0 to 100 based on the wound healing condition. **(B)** The example sample for VAS scoring.

Fig. 5. FMOD and F06-C40 reduce scar formation in adult red Duroc pig wounds.

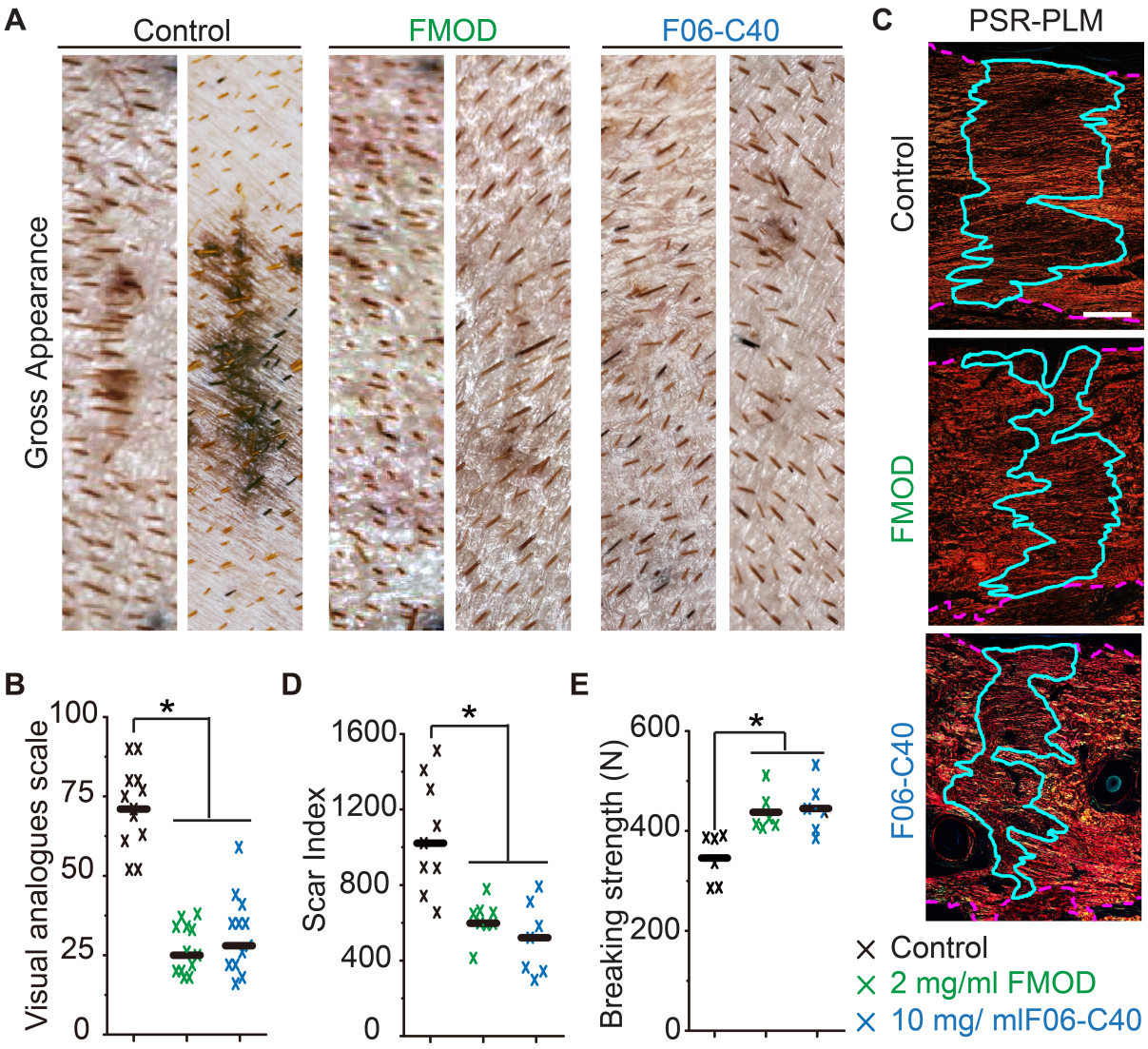

Fig. 5. F06-C40 reduces scar formation in adult red Duroc pig wounds. 1.5-cm length (0.5-cm width) primarily closed wounds (modified incisional) were created on adult female red Duroc pig dorsal skin. 100 µl of 2.0 mg/ml recombinant human FMOD (whole protein), 10.0 mg/ml F06-C40 peptide, or PBS control was intradermally injected into each wound edge at time 0 with another 50 µl injection into each wound edge 24 hours later. **(A)** Representative scar appearance at 8 weeks post-injury. **(B)** Visual Analogue Scale scoring of scar appearance, as determined by three blinded MD reviewers. Lower values indicate subjective improvements in scar appearance (N = 2 pigs). **(C)** PSR-polarized microscope (PLM). Scale bar = 0.5 mm. **(D)** Quantification of 8-week scar size among treatment groups. FMOD and F06-C40 showed similar efficacy in scar size reduction as measured by Scar Index. **(D)** Tensile strength testing at 8 weeks showed significantly increased breaking strength in FMOD and F06-C40 wounds. N = 12 wounds per treatment, N = 2 pigs. *p < 0.05.

3.3 F06-C40 reduces high-tension scarring in red Duroc pig models.

To explore the efficacy of F06-C40 on high-tension wounds, a large wound model was created with width of the elliptically excised, full-thickness wound 4 folds of normal incisional wound from 0.5 cm width (1.5-cm length) to 2.0 cm width **(Fig. 6A)**. Strikingly, the scar appearance was highly improved with F06-C40 injection **(Fig. 6C, 6D)**. F06-C40 application also significantly reduced scar size with the quantification of SI, which showed 46% size reduction **(Fig. 6E, 6F)**, while breaking strength increased by 160% in the high tension wound **(Fig. 6B)**.

Collectively, all preclinical studies to date demonstrate that FMOD effectively reduces scar in both normal and hypertrophic scar models, while increasing tensile strength.

Fig. 6. F06-C40 reduces scars in high-tension red Duroc pig wounds.

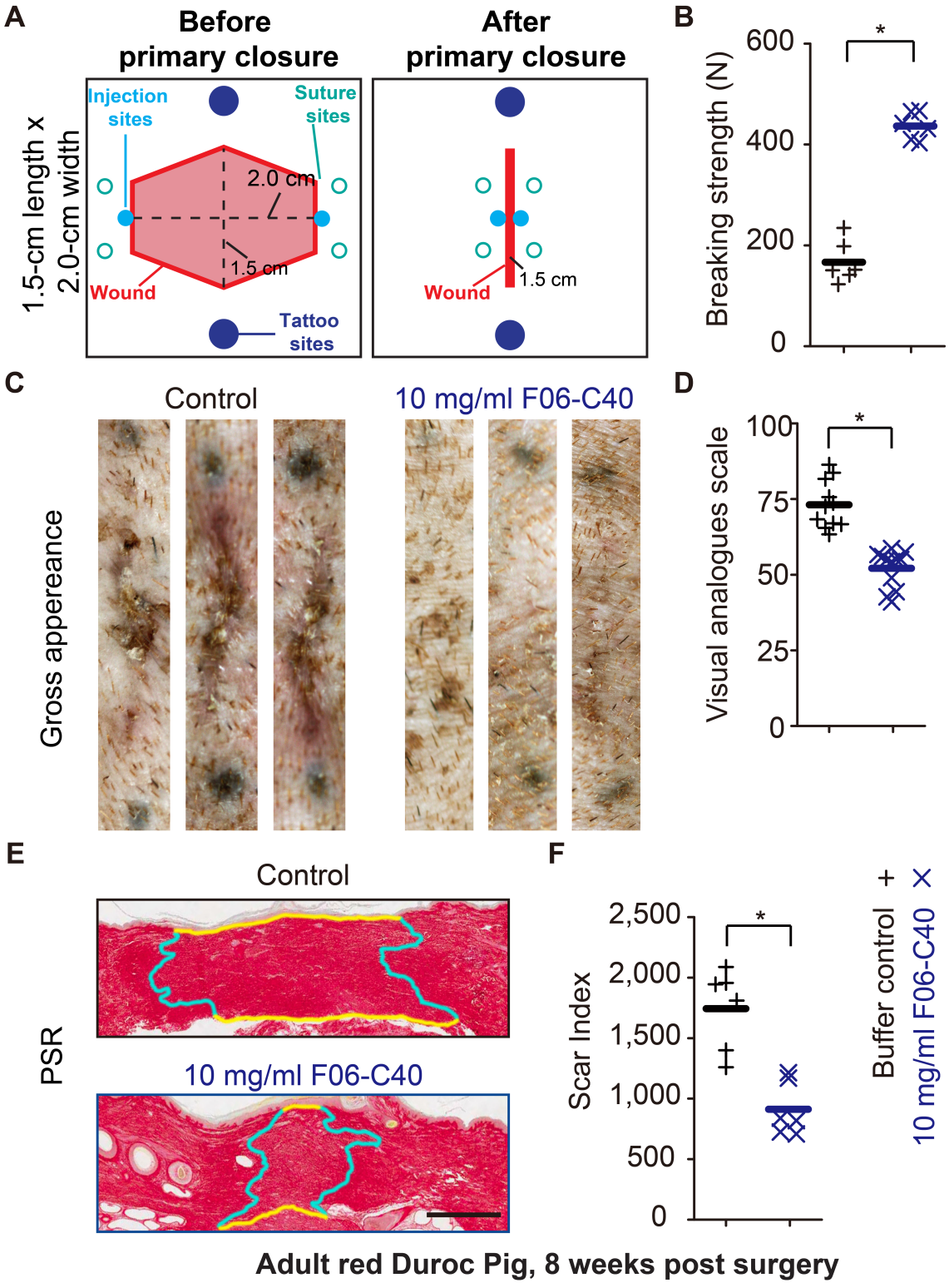

Fig. 6. F06-C40 reduces scars in high-tension red Duroc pig wounds. (A) 1.5-cm length (2.0-cm width) primarily closed wounds (modified incisional) were created on adult female red Duroc pig dorsal skin. 100µl of 10.0 mg/ml F06-C40 peptide or control buffer was intradermally injected into each wound edge at time 0. **(B)** Tensile strength testing at 8 weeks showed significantly increased breaking strength in F06-C40 wounds. **(C)** Gross appearance of the wounds was determined by **(D)** VAS scoring with three-blinded MD reviewers. Lower values indicate subjective improvements in scar appearance. **(E)** Scar was also stained with picrosirius red (PSR). **(F)** Quantification of 8-week scar size among treatment groups showed peptide significantly reduced scar formation as measured by Scar Index. N = 2 pigs. *P < 0.05.

3.4 Nontoxicity of F06-C40 in Yorkshire pig models

F06-C40 showed efficacy for wound healing, while being easy and inexpensive to be produced. To investigate the toxicity of F06-C40, we evaluated the immunoreaction after F06-C40 injection into Yorkshire pigs. Yorkshire pigs were injected with F06-C40 at the concentrations up to 50 mg/ml with 0.3 ml applied for 1.5-cm linear wound. Clinical observation and body weight were assessed daily. In 12 weeks, we did not observe any undesired immune response, local toxicity, or pathology with F06-C40 injection. The number of CD45 T cells, macrophages and mast cells were similar in control and peptide groups **(Fig. 7)**, indicating the nontoxicity of F06-C40 in pig models.

Fig. 7. Toxicity studies of F06-C40 on Yorkshire pig models.

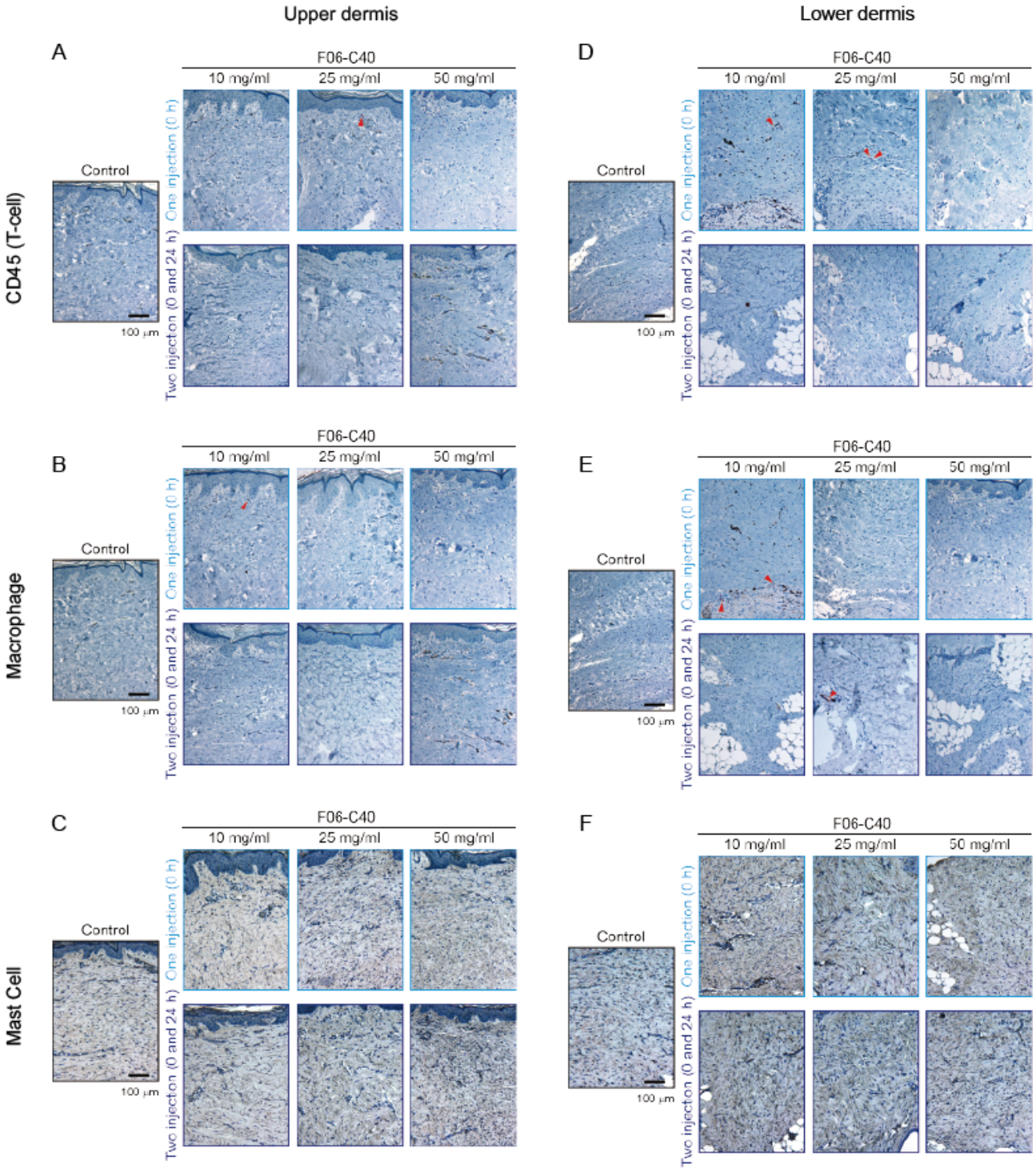

Fig. 7 Toxicity studies of F06-C40 on Yorkshire pig models. 1.5-cm length (0.5-cm width) primarily closed wounds in Yorkshire pigs were treated with F06-C40 at times 0 and 24 hours by intradermal injection. We locally tested F06-C40 concentrations from 10 mg/ml up to 50 mg/ml with 0.3 ml applied for 1.5-cm linear wound. Compared with control, the pig primary wound closure model did not show local toxicity with similar number of CD45 T-cells **(A; D)**, macrophages **(B; E)**, and mast cells **(C; F)** in upper and lower dermis at 12 weeks. N = 12 wounds per treatment, N = 5 pigs. Scale bar = 100 μm.

DISCUSSION

In the present study, the efficacy of FMOD and F06-C40 was tested in large animal acute wound models. Consistent with our previous findings in small animal models, the results from this study demonstrated the ability of FMOD and F06-C40 to reduce normal scars and hypertrophic scars in porcine models.

FMOD and F06-C40 application potently reduced adult scar formation in large animal acute wound models while increasing tensile strength and improving dermal collagen organization. In the normal wound healing models, FMOD and F06-C40 application significantly reduced scar by improving the gross appearance, accelerating wound healing process, and improving collagen architecture. They also increased tensile strength in normal wound healing pigs. The optimized dose and regimen for F06-C40 (10mg/ml with one injection) were used in further experiments. To explore possible applications for FMOD and F06-C40 peptide, red Duroc pig models were used to simulate a human hypertrophic scar scenario. Similarly, the gross appearance, and ECM organization of scars were pronouncedly improved, and scar area was reduced with the injection of FMOD or F06-C40 in both normal hypertrophic scars and high-tension hypertrophic scars. The successful decrease of scar formation in FMOD- and F06-C40-treated groups indicated they have the potential to treat human hypertrophic scarring. CLP is the most common craniofacial congenital anomaly present at birth in the US[1]. One of the difficulties to treat CLP is due to the high tension in the suture line[52]. F06-C40 successfully reduced scar formation in high-tension red Duroc pig wound models, indicating the therapeutic potential for CLP treatment.

As a protein in a family of SLRPs, which also includes decorin, biglycan, and

lumican, FMOD can be found in the epidermis and is essential for fetal scarless wound healing, collagen architecture, scar formation, and angiogenesis after injuries[40,43-45,53]. It is highly expressed in the skin of scarless fetal wounds. FMOD has critical roles in ECM assembly, organization, and degradation as well as ability to bind latent and active TGF-β1[36,38,49,54]. FMOD application significantly decreases rat and mouse wound scarring. And the deficiency of FMOD can lead to deficient fibroblast migration/invasion, deficient myofibroblast differentiation and contraction, and delayed wound closure[43,53]. F06-C40, as a shorter FMOD-derived peptide, maintains the anti-scar effect and has similar biological effects as FMOD, while being much more rapid and inexpensive to generate. At the cellular level, the application of FMOD and F06-C40 peptide increases dermal fibroblast migration and invasion and myofibroblast differentiation and contraction, according to previous studies[55]. In addition, FMOD and F06-C40 peptide increase early CTGF expression. The changes in the cellular level, such as increased fibroblast migration/invasion and myofibroblast differentiation /contraction, promote timely wound closure and result in strong early wound contraction, less ECM deposition, decreased inflammation, and decreased scar size. Furthermore, previous studies have shown that FMOD is the mediator for TGF-β1, which has been implicated in a growing number of fibrotic pathologies such as keloids and hypertrophic scars[56-58]. Based on previous studies and our present work demonstrating the anti-scar effect of FMOD and F06-C40 on different pig models with multiple wound scenarios, we predict that the anti-scar effect of FMOD and F06-C40 peptide results from the changes on fibroblast and myofibroblast after treatment. In addition, the modulating effect on TGF-β1 decreases fibrotic pathologies in hypertrophic scar models.

Taken together, our current study has high clinical impact and significantly advances the field of wound healing and regeneration, highlighting FMOD and F06-C40 as novel pharmaceutical candidates for enhancing adult cutaneous wound healing in humans. Remarkably, applying FMOD and F06-C40 on pig wound models reduced not only normal scarring, but also hypertrophic scar formation in a high-tension circumstance. Meanwhile, the toxicity studies confirmed the safety for F06-C40 application **(Fig. 7)**. The efficacy of F06-C40 in reducing scars, together with its production efficiency and safety profiles, makes F06-C40 a promising drug for wound healing and scar reducing. Recently, the anti-scar property of F06-C40 was successfully confirmed in diabetic mouse wound models. Use of FMOD and F06-C40 may represent the first successful attempt to 'turn back the clock' the natural transition from fetal scarless healing to adult repair with scarring. Further investigation is warranted to mechanistically elucidate how FMOD and F06-C40 modulates molecular pathways to achieve fetal-type scarless wound repair in adults.

REFERENCES

1. Sund, B. *New developments in wound care.*, 1-255 (PJB Publications, 2000).

2. Eming, S.A., Martin, P. & Tomic-Canic, M. Wound repair and regeneration: mechanisms, signaling, and translation. *Sci Transl Med* **6**, 265sr6 (2014).

3. Hamilton, B.E., Martin, J.A., Osterman, M.J., Curtin, S.C. & Matthews, T.J. Births: Final Data for 2014. *Natl Vital Stat Rep* **64**, 1-64 (2015).

4. Baker, R., Urso-Baiarda, F., Linge, C. & Grobbelaar, A. Cutaneous scarring: a clinical review. *Dermatol Res Pract* **2009**, 625376 (2009).

5. Profyris, C., Tziotzios, C. & Do Vale, I. Cutaneous scarring: Pathophysiology, molecular mechanisms, and scar reduction therapeutics Part I. The molecular basis of scar formation. *J Am Acad Dermatol* **66**, 1-10; quiz 11-2 (2012).

6. Masters, M., McMahon, M. & Svens, B. Reliability testing of a new scar assessment tool, Matching Assessment of Scars and Photographs (MAPS). *J Burn Care Rehabil* **26**, 273-84 (2005).

7. van Zuijlen, P.P. *et al.* Collagen morphology in human skin and scar tissue: no

adaptations in response to mechanical loading at joints. *Burns* **29**, 423-31 (2003).

8. Khorasani, H. *et al.* A quantitative approach to scar analysis. *Am J Pathol* **178**, 621-8 (2011).

9. Mostaco-Guidolin, L.B. *et al.* Collagen morphology and texture analysis: from statistics to classification. *Sci Rep* **3**, 2190 (2013).

10. Son, D. & Harijan, A. Overview of surgical scar prevention and management. *J Korean Med Sci* **29**, 751-7 (2014).

11. Goel, A. & Shrivastava, P. Post-burn scars and scar contractures. *Indian J Plast Surg* **43**, S63-71 (2010).

12. Aarabi, S., Longaker, M.T. & Gurtner, G.C. Hypertrophic scar formation following burns and trauma: new approaches to treatment. *PLoS Med* **4**, e234 (2007).

13. Zhu, K.Q., Carrougher, G.J., Gibran, N.S., Isik, F.F. & Engrav, L.H. Review of the female Duroc/Yorkshire pig model of human fibroproliferative scarring. *Wound Repair Regen* **15 Suppl 1**, S32-9 (2007).

14. Rabello, F.B., Souza, C.D. & Farina Junior, J.A. Update on hypertrophic scar

treatment. *Clinics (Sao Paulo)* **69**, 565-73 (2014).

15. Zhu, K.Q. *et al.* The female, red Duroc pig as an animal model of hypertrophic scarring and the potential role of the cones of skin. *Burns* **29**, 649-64 (2003).

16. Linares, H.A., Kischer, C.W., Dobrkovsky, M. & Larson, D.L. The histiotypic organization of the hypertrophic scar in humans. *J Invest Dermatol* **59**, 323-31 (1972).

17. Raj Mani, M.R., Vijay Shukla. *Measurements in Wound Healing: Science and Practice*, 40 (Springer Science & Business Media, 2012).

18. Suvik A, E.A.W.M. The Use of Modified Masson's Trichrome Staining in Collagen Evaluation in Wound Healing Study. *Malaysian Journal of Veterinary Research* **3**, 9 (2012).

19. Katz, M.Y. *et al.* Three-dimensional myocardial scarring along myofibers after coronary ischemia-reperfusion revealed by computerized images of histological assays. *Physiol Rep* **2**(2014).

20. Wilgus, T.A., Bergdall, V.K., Dipietro, L.A. & Oberyszyn, T.M. Hydrogen peroxide

disrupts scarless fetal wound repair. *Wound Repair Regen* **13**, 513-9 (2005).

21. Liu, T., Xu, Y., Sun, D. & Xie, L. Histological evaluation of corneal scar formation in pseudophakic bullous keratopathy. *PLoS One* **7**, e39201 (2012).

22. Vogel, B., Siebert, H., Hofmann, U. & Frantz, S. Determination of collagen content within picrosirius red stained paraffin-embedded tissue sections using fluorescence microscopy. *MethodsX* **2**, 124-34 (2015).

23. S., B. A modified Picro-Sirius Red (PSR) staining procedure with polarization microscopy for identifying collagen in archaeological residues. *Journal of Archaeological Science* **61**, 8 (2015).

24. Corr, D.T. & Hart, D.A. Biomechanics of Scar Tissue and Uninjured Skin. *Adv Wound Care (New Rochelle)* **2**, 37-43 (2013).

25. Buffoni, F. *et al.* Skin wound healing: some biochemical parameters in guinea-pig. *J Pharm Pharmacol* **45**, 784-90 (1993).

26. Dorsett-Martin, W.A. Rat models of skin wound healing: a review. *Wound Repair Regen* **12**, 591-9 (2004).

27. Dunn, L. *et al.* Murine model of wound healing. *J Vis Exp*, e50265 (2013).

28. Wang, X., Ge, J., Tredget, E.E. & Wu, Y. The mouse excisional wound splinting model, including applications for stem cell transplantation. *Nat Protoc* **8**, 302-9 (2013).

29. Sullivan, T.P., Eaglstein, W.H., Davis, S.C. & Mertz, P. The pig as a model for human wound healing. *Wound Repair Regen* **9**, 66-76 (2001).

30. Seaton, M., Hocking, A. & Gibran, N.S. Porcine models of cutaneous wound healing. *ILAR J* **56**, 127-38 (2015).

31. Lee, P.Y. *et al.* Proteomic analysis of pancreata from mini-pigs treated with streptozotocin as a type I diabetes models. *J Microbiol Biotechnol* **20**, 817-20 (2010).

32. Richardson, M.R., Lai, X., Dixon, J.L., Sturek, M. & Witzmann, F.A. Diabetic dyslipidemia and exercise alter the plasma low-density lipoproteome in Yucatan pigs. *Proteomics* **9**, 2468-83 (2009).

33. Meurens, F., Summerfield, A., Nauwynck, H., Saif, L. & Gerdts, V. The pig: a

model for human infectious diseases. *Trends Microbiol* **20**, 50-7 (2012).

34. Zhu, K.Q. *et al.* Further similarities between cutaneous scarring in the female, red Duroc pig and human hypertrophic scarring. *Burns* **30**, 518-30 (2004).

35. Antonsson, P., Heinegard, D. & Oldberg, A. Structure and deduced amino acid sequence of the human fibromodulin gene. *Biochim Biophys Acta* **1174**, 204-6 (1993).

36. Oldberg, A., Antonsson, P., Lindblom, K. & Heinegard, D. A collagen-binding 59-kd protein (fibromodulin) is structurally related to the small interstitial proteoglycans PG-S1 and PG-S2 (decorin). *EMBO J* **8**, 2601-4 (1989).

37. Soo, C. *et al.* Differential expression of fibromodulin, a transforming growth factor-beta modulator, in fetal skin development and scarless repair. *Am J Pathol* **157**, 423-33 (2000).

38. Merline, R., Schaefer, R.M. & Schaefer, L. The matricellular functions of small leucine-rich proteoglycans (SLRPs). *J Cell Commun Signal* **3**, 323-35 (2009).

39. Hassan, D.A., Samy, R.M., Abd-Elrahim, O.T. & Salib, C.S. Study of fibromodulin

gene expression in B-cell chronic lymphocytic leukemia. *J Egypt Natl Canc Inst* **23**, 11-5 (2011).

40. Zheng, Z. *et al.* Reprogramming of human fibroblasts into multipotent cells with a single ECM proteoglycan, fibromodulin. *Biomaterials* **33**, 5821-31 (2012).

41. Svensson, L. *et al.* Fibromodulin-null mice have abnormal collagen fibrils, tissue organization, and altered lumican deposition in tendon. *J Biol Chem* **274**, 9636-47 (1999).

42. Lee, Y.H. & Schiemann, W.P. Fibromodulin suppresses nuclear factor-kappaB activity by inducing the delayed degradation of IKBA via a JNK-dependent pathway coupled to fibroblast apoptosis. *J Biol Chem* **286**, 6414-22 (2011).

43. Zheng, Z. *et al.* Delayed wound closure in fibromodulin-deficient mice is associated with increased TGF-beta3 signaling. *J Invest Dermatol* **131**, 769-78 (2011).

44. Jian, J. *et al.* Fibromodulin promoted in vitro and in vivo angiogenesis. *Biochem Biophys Res Commun* **436**, 530-5 (2013).

45. Zheng, Z. *et al.* Fibromodulin Enhances Angiogenesis during Cutaneous Wound Healing. *Plast Reconstr Surg Glob Open* **2**, e275 (2014).

46. Kapoor, M. *et al.* Connective tissue growth factor promoter activity in normal and wounded skin. *Fibrogenesis Tissue Repair* **1**, 3 (2008).

47. Hinz, B. Formation and function of the myofibroblast during tissue repair. *J Invest Dermatol* **127**, 526-37 (2007).

48. Tomasek, J.J., Gabbiani, G., Hinz, B., Chaponnier, C. & Brown, R.A. Myofibroblasts and mechano-regulation of connective tissue remodelling. *Nat Rev Mol Cell Biol* **3**, 349-63 (2002).

49. Hildebrand, A. *et al.* Interaction of the small interstitial proteoglycans biglycan, decorin and fibromodulin with transforming growth factor beta. *Biochem J* **302 (Pt 2)**, 527-34 (1994).

50. Gurtner, G.C. *et al.* Improving cutaneous scar formation by controlling the mechanical environment: large animal and phase I studies. *Ann Surg* **254**, 217-25 (2011).

51. Duncan, J.A. *et al.* Visual analogue scale scoring and ranking: a suitable and sensitive method for assessing scar quality? *Plast Reconstr Surg* **118**, 909-18 (2006).

52. Ellore, V.P. *et al.* Pre: Surgical orthopedic pre-maxillary alignment in bilateral cleft lip and palate patient. *Contemp Clin Dent* **3**, 359-62 (2012).

53. Zheng, Z. *et al.* Fibromodulin-deficiency alters temporospatial expression patterns of transforming growth factor-beta ligands and receptors during adult mouse skin wound healing. *PLoS One* **9**, e90817 (2014).

54. Ameye, L. & Young, M.F. Mice deficient in small leucine-rich proteoglycans: novel in vivo models for osteoporosis, osteoarthritis, Ehlers-Danlos syndrome, muscular dystrophy, and corneal diseases. *Glycobiology* **12**, 107R-16R (2002).

55. Zheng, Z.Y., W.; Zara J.; Wang J.; Zhang, X.; Ting, K.; Soo, C. The role of fibromodulin in fibroblast migration and enhanced wound closure. *Journal of the American College of Surgeons* **211**(2010).

56. Bayat, A., Bock, O., Mrowietz, U., Ollier, W.E. & Ferguson, M.W. Genetic

susceptibility to keloid disease and hypertrophic scarring: transforming growth factor beta1 common polymorphisms and plasma levels. *Plast Reconstr Surg* **111**, 535-43; discussion 544-6 (2003).

57. Rorison, P. *et al.* Longitudinal changes in plasma Transforming growth factor beta-1 and post-burn scarring in children. *Burns* **36**, 89-96 (2010).

58. Bayat, A., McGrouther, D.A. & Ferguson, M.W. Skin scarring. *BMJ* **326**, 88-92 (2003).